Modelling of Solid State Bonding Process by Power Law Creep

Yasuo TAKAHASHI*, Katsunori INOUE, Kimiyuki NISHIGUCHI† and Tsutomu KOGUCHI††**

Abstract

The model of solid state bonding based on the finite element method is proposed. It is assumed that the bonding (adhering) process is controlled by viscoplastic (power law creep) deformation. This finite element method can be applied to the large deformation processes, in which the strain rate dependence is taken into account. The numerical results agrees with the experimental ones. We further discuss different models proposed by several researchers, comparing them with the finite element model with respect to the void shrinking rate. It is found that the applicability of the solid state bonding due to power law creep are limited by the degree of bulk deformation(value of strain rate), i.e., the void crushing rate is strikingly affected by the constraint condition of bulk. Therefore, we need to select the models in accordance with the situation of bulk deformation.

KEY WORDS : (Solid State Bonding), (Power Law Creep), (Modelling), (Finite Element Method)

Nomenclature

L_o : half pitch of surface asperity
h_{oo} : height of surface asperity
L : half void spacing
w : half void width
X : unit of bonded length and equivalent to area bonded if unit thickness is considered
h : half void height
S : percentage bonded area ($= X/L$)
k : Boltzmann's constant
P : bonding pressure ($= | \sigma_B |$)
T : absolute temperature
t : time
V : void volume per unit thickness at time t
A_o : nondimensional constant for creep rate equation
G : shear modulus
b : Burgers vector
A : creep constant ($= A_o (D_v \cdot b \cdot G/kT)$)
A_p : plain strain creep constant ($= A (\sqrt{3}/2)^{n+1}$)
n : stress exponent of creep flow
Q_c : activation energy of creep flow
σ_B : gross stress (the sign for compressive stress is minus.)
σ_e : equivalent stress
σ_x : local stress in x direction parallel to the bonded interface ($= \sigma_a$)
σ_y : local stress in y direction normal to the bonded interface ($= \sigma_b$)
$\dot{\varepsilon}_\infty$: creep strain rate of bulk
$\dot{\varepsilon}_y$: local creep strain rate in y direction
$\dot{\varepsilon}_x$: local creep strain rate in x direction
$\dot{\varepsilon}_e$: equivalent strain rate

† Received on Nov,12,1991
* Associate professor
** Professor
† Professor, Faculty of Eng. Dept. of Weld. and Production Eng.
†† Graduate Student Osaka University, present address:Mitsubishi Heavy Industry

Transactions of JWRI is published by Welding Research Institute, Osaka University, Ibaraki, Osaka 567, Japan

1. Introduction

It is widely accepted that power law creep deformation makes an important role in solid state bonding and pressure sintering[1-3]. The power law creep mechanism is an operation for crushing a void on the bond interface by the surrounding matrix[4,5]. In order to quantitatively understand the contribution of the power law creep to void shrinkage, several different models have been developed individually[6-9]. Although all of the models take account of the power law creep, there is a severe difference between the bonding rates. This is because the origin of the models was different from each other; Wilkinson and Ashby[10] first proposed a void crushing model by power law creep which approximated to the creep of a thick spherical shell and was followed by Derby and Wallach[1] and Takahashi et al.[3,9], who corrected Wilkinson's model for a cylindrical void in order to apply it to the diffusion bonding for specimens with two dimensional surface asperities. On the other hand, Garmong et al.[11] proposed a slice surface asperity model, followed by Guo and Ridley[6]. In Wilkinson's shell model, the rate equation is different between earlier and latter half of sintering[9], while the rate equation of Guo's slice model is the same between the earlier and latter half. As stated below, the void shrinkage rate of Wilkinson's model is quite different to that of Guo's model in the latter half of bonding. Hancock[12] developed a void growth model of power law creep, which had originally been proposed by McClintock[13]. Hancock's model was used by Hill and Wallach[8] to develop a diffusion bonding model. Many models of solid state bonding adopted one of these three models as power law creep mechanism. This is a reason why there is a severe difference between the bonding rates. Unless this is understood, it seems to be false to apply the void shrinkage models for predicting the solid state bonding. However, there are few studies which discuss the difference between models[14]. Therefore, we need to discuss the solid state bonding processes given by different models, comparing them with one another. We have developed a numerical model of the solid state bonding by power law creep[15]. It is based on a finite element method. In the present paper, we introduce it and compare it with the other recent models. We further discuss the applicability of the models, i.e, we describe the proper conditions of bulk deformation for each model.

2. Geometry of bond interface

Figure 1 shows the schematic illustration (cross section) of the faying surfaces and the void arranged at regular interval $2L$. We assume that the faying surfaces are treated as a two dimensional shape consisting of long triangular ridges with regular peaks (Fig. 1 (a)), in order to eliminate complex boundary conditions concerning void shape. Two faying surfaces are contacted peak to peak. This local contact is achieved by instantaneous plastic deformation[3,4,9], resulting in a two dimensional arrange of voids as shown in Fig. 1 (b). The initial contact X_o is given by the slip line analysis if X_o is small enough (P is

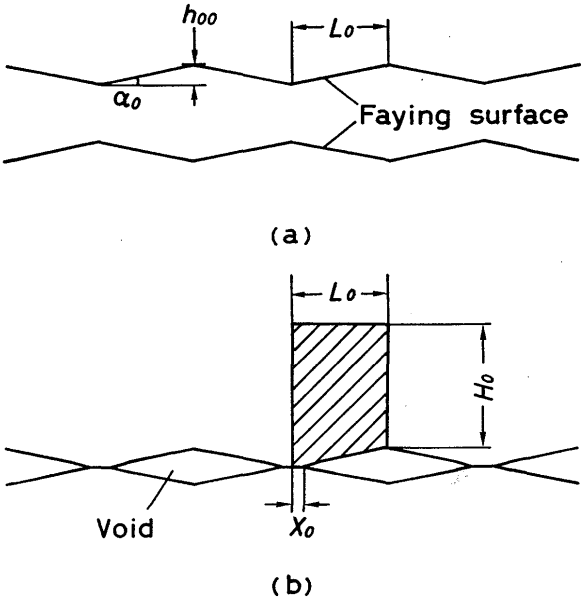

Fig. 1 Schematic illustration of geometry of faying surface and bonded interface. (a) faying surface, (b) void arranged in a regular interval.

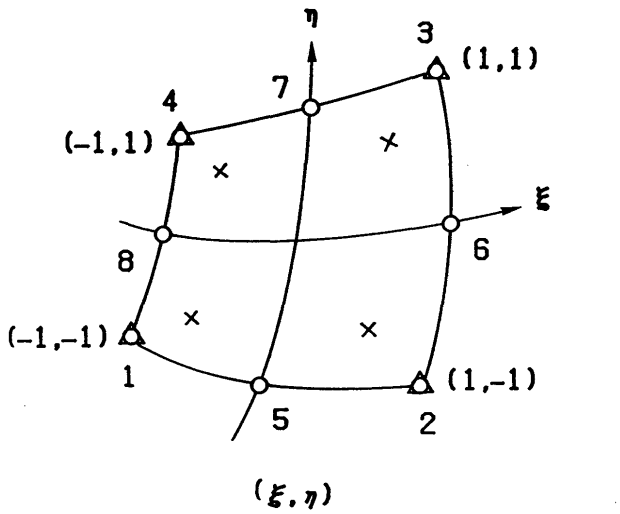

Fig. 2 A two dimensional element with eight nordal points.

small enough)[16]. We treated it as $X_o = 0.15\ L_o$ when P is high enough, assuming that the bonded area X is instantly attained to 15% of L_o.

After this, the power law creep only contribute to the bonding process.

3. A Finite Element Model

Figure 2 shows a two dimensional element adopted in the present study. This element has eight nodal points and can be applied to large deformation problem. The position inside each element is represented by a local coordinate (ξ , η) and a overall coordinate (x, y) as detailed elsewhere[15]. The area indicated by oblique lines in Fig. 1 (b) was modeled by the finite elements as shown in **Fig. 3** (a). The value of H_o indicated in Fig. 1 (b) were set to be five times as large as h_{oo}. Two types of constraint conditions were adopted. One of them was a perfect constraint condition, that is, we assumed that $\dot{u}_x = 0$ at $x = L_o$. In the other, we assumed that the bulk is uniformly deformed.

Numerical solutions were obtained by the perturbation theory which assumed the initial displacement vector $\{\dot{u}\}$ and solved the perturbation $\Delta\{\dot{u}\}$. The flow chart of the viscoplastic finite element method (FEM) is shown in **Fig. 4**. When the void surface reached the bond-interface (x axis, $y = 0$), we treated it as a "folding" phenomenon which we can see in Fig. 3 (b). Also, we modified the mesh division if a parameter of IFOLD is greater than four.

4. Calculated results by FEM

Figures 5 and **6** show the numerical results. The bonding progresses in alphabetical order. Figure 5 is for the perfect constraint condition and Fig. 6 for the uniform deformation condition. The nodal points at the void surface is folded one by one. We find that the initial bonded area at $t = 0$ s cannot expand as much as we expected even for the uniform deformation condition. In the earlier stage of bonding process ($S < 50\%$), the bonding rates for constraint conditions are not so smaller than those of uniform deformation conditions, while the former is much smaller than the latter in $S > 50\%$. It is found that the constraint condition cannot so influence the bonding process in the earlier half of bonding. As we can see in Figs. 5 and 6, the FEM model developed in the present study makes it possible to comprehend the behaviour of the void crushed by the surrounding matrix.

Figure 7 shows the change of percent bonded area $S(= X/L)$ with time, together with the experimental results ($h_{oo} \sim 2\ \mu$m, $L_o \sim 10\ \mu$m). We cannot ignore the low

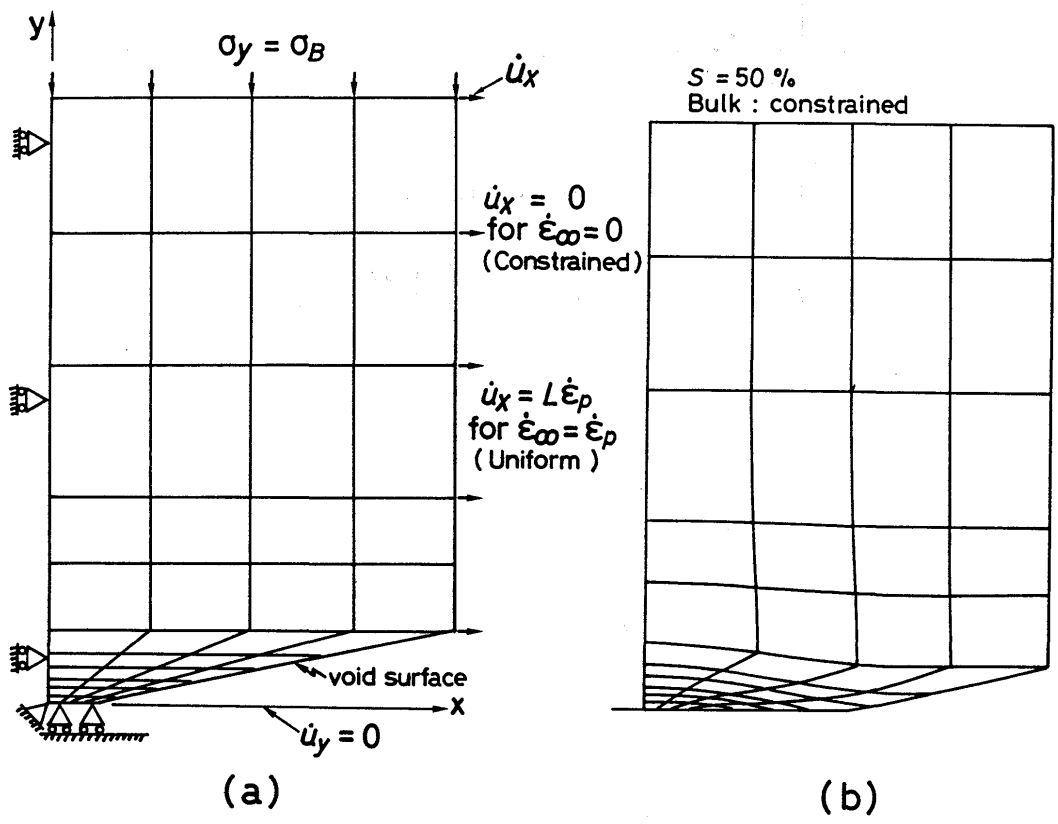

Fig. 3 Boundary condition for FEM (a) and deformed mesh pattern (b).

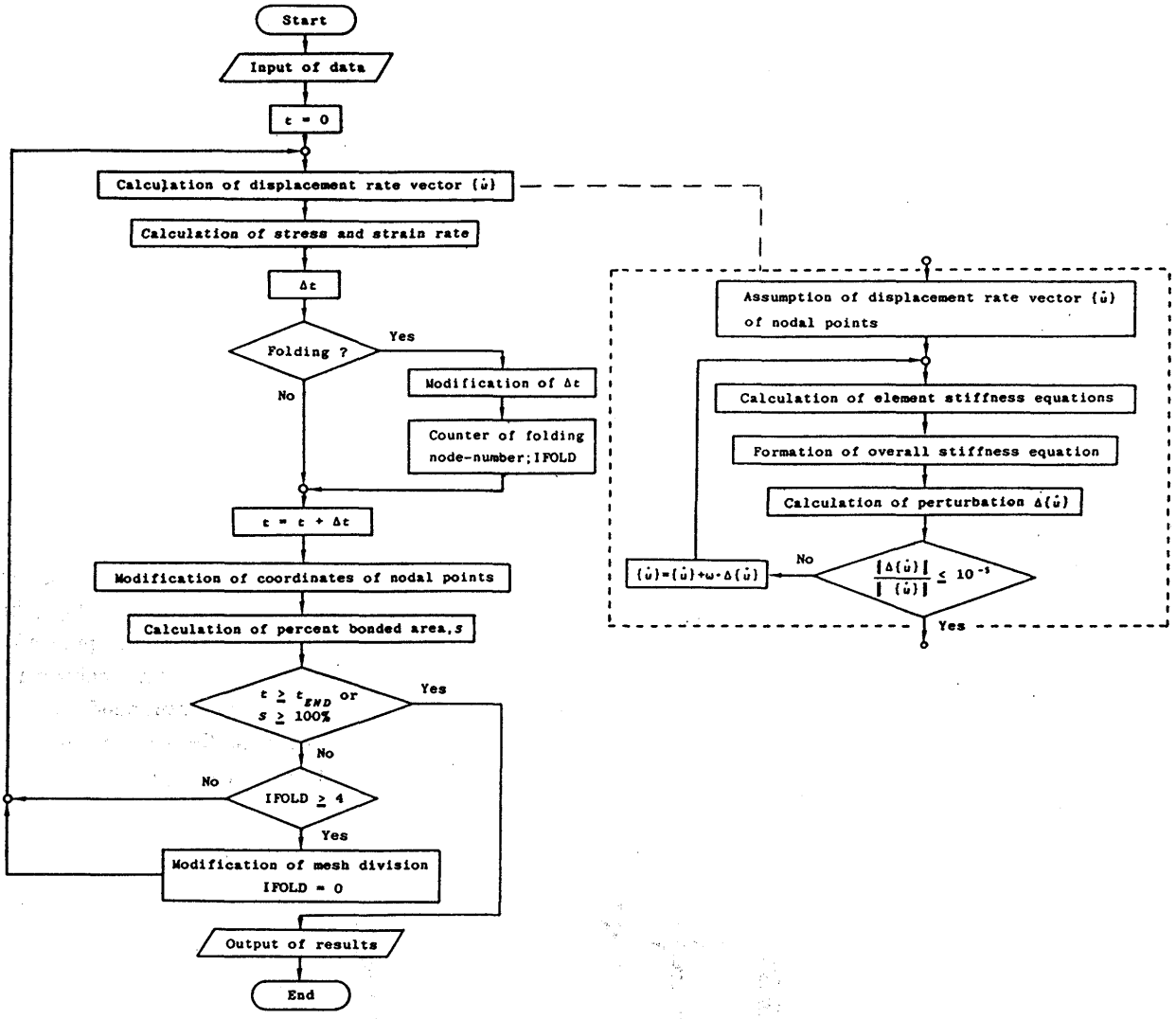

Fig. 4 Flow chart of visco-plastic finite element method.

temperature creep for the test condition of $T = 973$ K. Thus, in Fig. 7, we assumed that total creep rate $\dot{\varepsilon}_t$ is given by $\dot{\varepsilon}_L + \dot{\varepsilon}_H$, where $\dot{\varepsilon}_L$ and $\dot{\varepsilon}_H$ are, respectively, low and high temperature type creep rates. The value of their constants used in the numerical calculations are shown in **Table 1**. The rate equation is expressed by eq. (24). It is found that the constraint of bulk restrains the bonding process strikingly. Also, the numerical model can predict the experimental results.

5. Analytical models and their characteristics

Let us introduce three kinds of void crushing models developed by several researchers in recent years. We need to lead the rate equations of the models for the same boundary condition (a rhombic shape void) to compare them with the FEM model.

5.1 Takahashi's model

Takahashi et al.[3,4,9] modified Wilkinson and Ashby's model[10] to apply it to plain strain void shrinkage process. The growth rate of unit of bonded length, X, is expressed by

$$\dot{X} = \frac{A_P \cdot X}{\{1 - (X/L)^{2/n}\}^n} \left\{ \frac{2 \cdot |\sigma_B|}{nG} \left(\frac{L}{X} - 1 \right) \right\}^n \quad (1)$$

for $S \leqq 50\%$ and

$$\dot{X} = \frac{A_P \cdot w}{\{1 - (w/L)^{2/n}\}^n} \left\{ \frac{2 \cdot |\sigma_B|}{nG} \right\}^n \quad (2)$$

for $S \geqq 50\%$. Because the void shape is rhombic, the change rate of half the void height is given by

$$\dot{h} = -h \cdot \dot{X} / (L + X) \quad (3)$$

from mass conservation[4]. Because $V = 2hw$ and $\dot{w} = -\dot{X}$, we obtain the void shrinkage rate given by

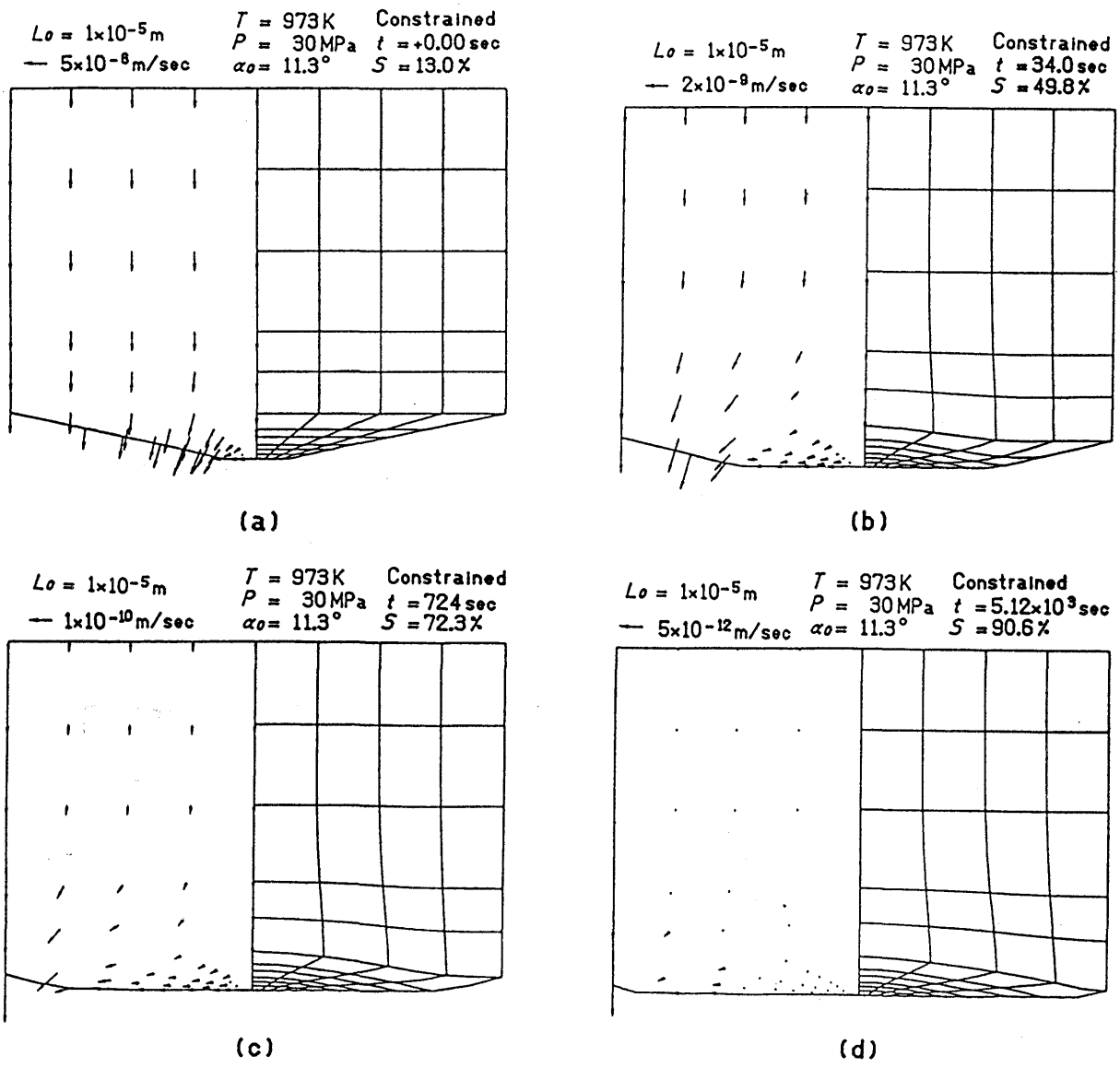

Fig. 5 Calculated results of the finite element model (the external condition: constrained). The bonding progresses in alphabetical order.

$$\dot{V} = 2\dot{h}w + 2h\dot{w}. \tag{4}$$

Equation (1) is applicable when the bulk is freely deformed. On the other hand, eq. (2) is valid when the bulk constrained as stated below (cf. **Figs. 8** and **9**).

5.2 Guo and Ridley's model

Guo and Ridley divided the matrix adjacent to the bonded interface into N slices with the thickness of δ_y, according to Garmong et al. ($\delta_y = h/N$)[19]. They assumed that the i th slice is uniformly deformed. Let us deduce the rate equation for rhombic void. Because we assume a plain strain condition, $\dot{\varepsilon}_{x_i} + \dot{\varepsilon}_{y_i} = 0$, i. e., $\dot{\varepsilon}_{y_i} = -\dot{\varepsilon}_{x_i} = -A_p (\sigma_i/G)^n$, where $\dot{\varepsilon}_{x_i}$ and $\dot{\varepsilon}_{y_i}$ are the strain rates of the i th slice in x and y directions, respectively. Also, the stress at the i th is given by $\sigma_i = (L/X_i)\ \sigma_B$, where X_i is half the width of the i th slice expressed by $X_i = \{(L - X)\ y_i + hX\}/h$ because of rhombic void. The change of the thickness of the i th slice, $\Delta\delta y_i$, for the time increment Δt is given by

$$\Delta\delta y_i = \dot{\varepsilon}_{yi} \cdot dt \cdot \delta_y = -A_p (\sigma_i/G)^n \cdot \Delta t\ \delta_y$$
$$= -A_p \left\{ \frac{L \cdot |\sigma_B|}{X_i \cdot G} \right\}^n \cdot \left(\frac{h}{N}\right) \Delta t. \tag{5}$$

Since the decrement of h is expressed by

$$\Delta h = \lim_{N\to\infty} \sum_{i=1}^{N} \Delta\delta y_i, \tag{6}$$

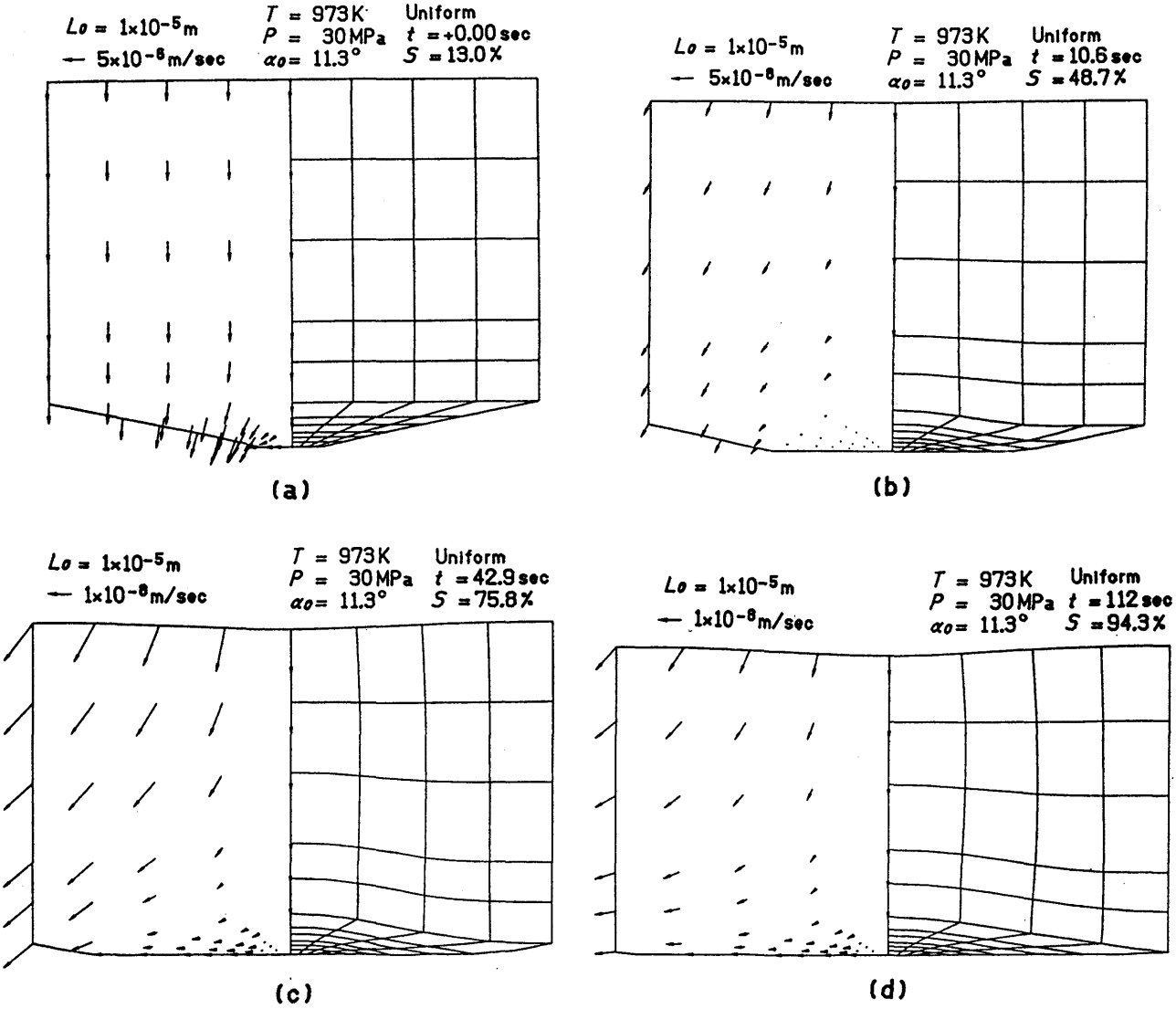

Fig. 6 Calculated results of the finite element model (the external condition: uniformly deformed bulk). The bonding progresses in alphabetical order.

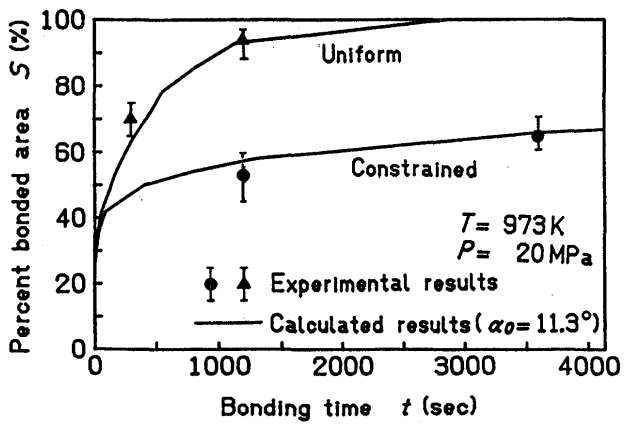

Fig. 7 Change in percentage bonded area S with time and the experimental test results. In the numerical solution, we coupled LT creep with HT creep.

the change rate of h is obtained by

$$\dot{h} = -A_p\,(P/G)^n \cdot \lim_{N\to\infty} \sum_{i=1}^{N} (L/X_i)^n \cdot \delta_y \tag{7a}$$

$$= -A_p\,(P/G)^n \cdot \int_0^h \left(\frac{L}{x}\right)^n dy, \tag{7b}$$

where $x = \{(L - X)/h\}\, y + X$. Therefore, the change rate of h is obtained by

$$\dot{h} = -A_p \left(\frac{P}{G}\right)^n \cdot \int_0^h \left\{\frac{hL}{(L-X)\cdot y + hX}\right\}^n dy$$

$$= -A_p \left(\frac{P}{G}\right)^n \cdot \frac{hL}{(n-1)(L-X)} \cdot \left\{\left(\frac{L}{X}\right)^{n-1} - 1\right\}. \tag{8}$$

Table 1 Material parameters for copper.

	Prameters		Value
D_{vo}	: Frequency factor of D_v		$0.62\text{x}10^{-4}$ m^2/s
Q_v	: Activation energy of volume self-diffusion		207.8 kJ/mol
b	: Burgers vector		$2.56\text{x}10^{-10}$ m
n	: Stress exponent of power law creep	HT creep	6.0
		LT creep	8.0
A_o	: Nondimensional creep constant	HT creep	$2.0\text{x}10^{10}$
		LT creep	$4.0\text{x}10^{10}$
Q_c	: Activation energy for power law creep	HT creep	207.8 kJ/mol
		LT creep	104.8 kJ/mol
T_m	: Melting point		1356 K
$G(T)$	: Shear modulus absolute temperature T		$a_G(T/T_m)^2+b_G(T/T_m)+c_G$
a_G	: Coefficient for $G(T)$		$-4.7\text{x}10^{10}$ N/m^2
b_G	: Coefficient for $G(T)$		$1.3\text{x}10^{10}$ N/m^2
c_G	: Coefficient for $G(T)$		$4.6\text{x}10^{10}$ N/m^2

Note: $G(T)$ is after Köster[22].

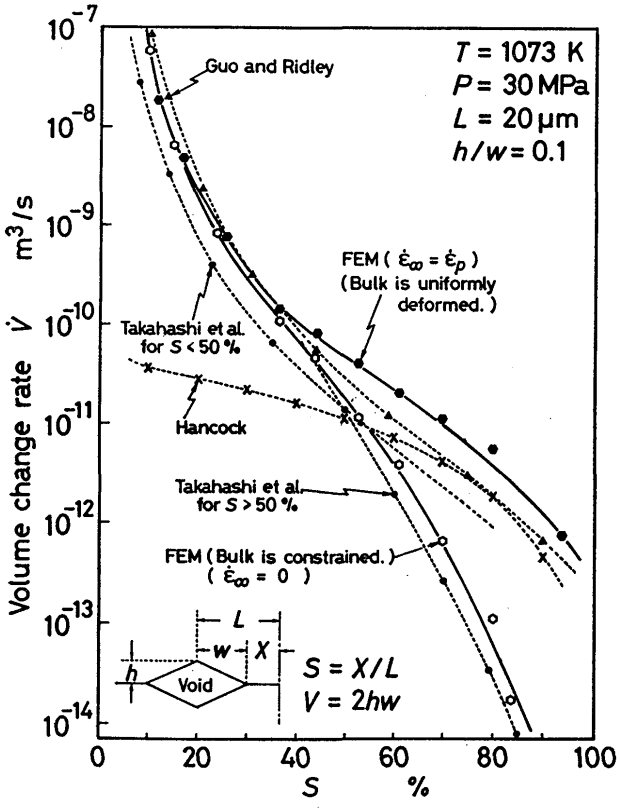

Fig. 8 Void volume change rate calculated by different models for power law creep mechanism.

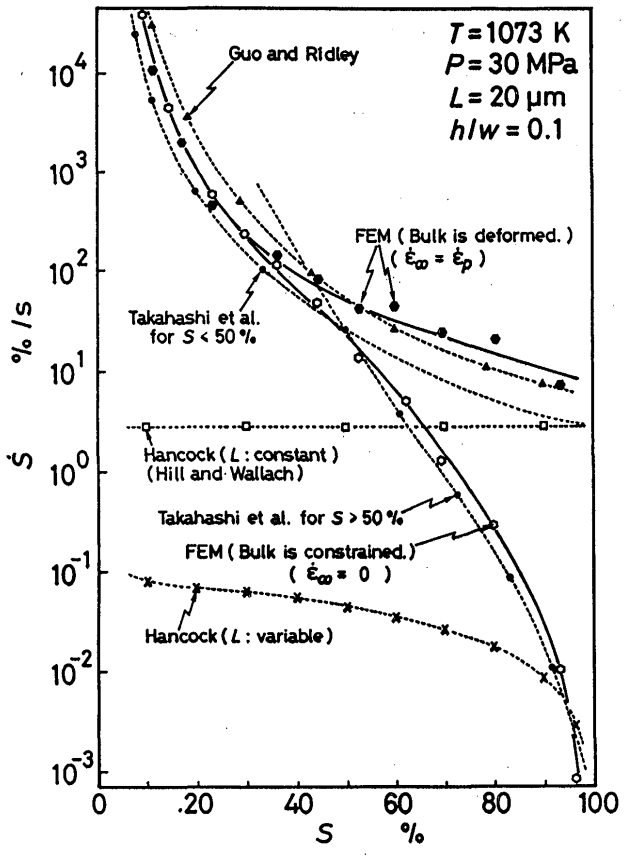

Fig. 9 Growth rate of percentage bonded area S estimated by different models for power law creep mechanism.

Also, the change rate of X is given by

$$\dot{X} = -\dot{h}\,(L + X)/h \tag{9}$$

from eq. (3). The volume change rate is given in same manner as eq. (4). We can obtain an analytical solution of eq. (8) without numerical integration, if we adopt a rhombic void. On the other hand, we need numerical integration for original Guo and Ridley's model of a lenticular void. However, there is little difference in value between eq. (8) in the present model and eq. (60) in Guo and Ridley's paper[6]. The present model is still called Guo and Ridley's model.

5.3 Hancock's model (Hill and Wallach's model)

Hill and Wallach[8] applied Hancock's model[12] to the void crushing process by power law creep. They had should take $\sigma_a\ (=\sigma_x) = 0$ and $\sigma_b\ (=\sigma_y) = -P$ in deriving the rate equation although it does not so matter in values. Here, σ_a and σ_b is referred to in appendix 4 of ref. (8) or ref. (13).

The equivalent strain and stress are, respectively, expressed by

$$\varepsilon_e = \left[\frac{2}{9}\{(\varepsilon_x - \varepsilon_y)^2 + (\varepsilon_y - \varepsilon_z)^2 + (\varepsilon_z - \varepsilon_x)^2\}\right]^{1/2}, \tag{10}$$

and

$$\sigma_e = \left[\frac{1}{2}\{(\sigma_x - \sigma_y)^2 + (\sigma_y - \sigma_z)^2 + (\sigma_z - \sigma_x)^2\}\right]^{1/2}, \tag{11}$$

where ε_i and σ_i ($i = x$, y, or z) are principal strain and stress, respectively. For plain strain condition, $\varepsilon_z = 0$ and $\gamma_{zx} = \gamma_{zy} = 0$ (γ_{ij} is shear strain). Also, $\sigma_z = (\sigma_x + \sigma_y)/2$, because the strain increment in the direction of z is expressed by

$$d\varepsilon_z = (d\varepsilon_e/\sigma_e)\cdot[\sigma_z - (1/2)(\sigma_x + \sigma_y)]. \tag{12}$$

According to McClintock[21],

$$\ln\left(\frac{R}{R_o}\right) = \frac{\sqrt{3}\cdot\varepsilon_e}{2\{1-(1/n)\}}\cdot \sinh\left\{\frac{\sqrt{3}\{1-(1/n)\}}{2}\cdot\frac{\sigma_x+\sigma_y}{\sigma_e}\right\} \tag{13}$$

and

$$M = \frac{\sigma_x-\sigma_y}{\sigma_x+\sigma_y} + \left(M_o - \frac{\sigma_x-\sigma_y}{\sigma_x+\sigma_y}\right)\cdot \exp\left\{-\frac{\sqrt{3}\cdot\varepsilon_e}{\{1-(1/n)\}}\cdot \sinh\left\{\frac{\sqrt{3}\{1-(1/n)\}}{2}\cdot\frac{\sigma_x+\sigma_y}{\sigma_e}\right\}\right\}, \tag{14}$$

where $R = (w + h)/2$, $R_o = (w_o + h_o)/2$, $M = (w - h)/(w + h)$, $M_o = (w_o - h_o)/(w_o + h_o)$. Because $\sigma_x = 0$ and $\sigma_y = \sigma_B(= -P)$ from the external condition and $\varepsilon_x = -\varepsilon_y$ from mass conservation ($\varepsilon_x + \varepsilon_y + \varepsilon_z = 0$), we obtain $\sigma_e = (\sqrt{3}/2)P$ and $(\sigma_x - \sigma_y)/(\sigma_x + \sigma_y) = (\sqrt{3}/2)(\sigma_x + \sigma_y)/\sigma_e = -1$. Because $\sinh(-x) = -\sinh(x)$, we can obtain

$$\ln(R/R_o) = -Z/2 \tag{15}$$

and

$$\ln(M + 1)/(M_o + 1) = Z, \tag{16}$$

where $Z = \{\sqrt{3}\,\varepsilon_e/(1 - n^{-1})\}\cdot\sinh(1 - n^{-1})$. The subscript o attached to w and h denotes the initial values of them, respectively. If eqs. (15) and (16) are differentiated with respect to time, we obtain

$$\dot{R}/R = -\dot{Z}/2 \tag{17}$$

and

$$\dot{M}/(M + 1) = \dot{Z}. \tag{18}$$

According to Hill and Wallach[8], $h = R(1 - M)$ and $w = R(1 + M)$ hold true. Thus, $\dot{h} = \dot{R}(1 - M) - R\dot{M}$ and $\dot{w} = \dot{R}(1 + M) + R\dot{M}$ is established. Therefore, we obtain

$$\dot{h} = -\left(\frac{h}{2} + w\right)\cdot\dot{Z} \tag{19}$$

and

$$\dot{w} = (w/2)\cdot\dot{Z}, \tag{20}$$

where $\dot{Z}$ is expressed by

$$\dot{Z} = \left\{\sqrt{3}\cdot\dot{\varepsilon}_e/\left(1 - \frac{1}{n}\right)\right\}\cdot \sinh\left(1 - \frac{1}{n}\right). \tag{21}$$

For the plain strain condition, $\dot{\varepsilon}_e$ is represented by

$$\dot{\varepsilon}_e = A\left(\frac{\sigma_e}{G}\right)^n = A\left(\frac{\sqrt{3}}{2}\right)^n\cdot\left(\frac{P}{G}\right)^n. \tag{22}$$

When L is variable, the change rate of L is expressed by

$$\dot{L} = L\cdot\dot{\varepsilon}_x = L\cdot\left(\frac{\sqrt{3}}{2}\right)\dot{\varepsilon}_e = LA_p\cdot\left(\frac{P}{G}\right)^n. \tag{23}$$

Also, the growth rate of S is given by $\dot{S} = (L\dot{w} - w\dot{L})/L^2$. However, eqs. (19) ~ (21) should be applied to the void shrinkage process of an isolated void, according to McClintock[13]. In other words, eqs. (19) ~ (21) should be used when $L \sim X >> w$. Hancock's model treats the void growth caused by the bulk deformation. L is changeable for the voids arranged in a regular interval.

The analytical models depend on the external condition, as mentioned above. Therefore, we need to understand the suitable condition for each model when we use it to predict the bonding process. In the following section, we will discuss their applicability, comparing them to the FEM model.

6. Applicability of models

The equivalent strain (creep) rate was given by

$$\dot{\varepsilon}_e = A_o \cdot \left(\frac{D_{ov}bG}{kT}\right) \cdot \exp\left(-\frac{Q_c}{RT}\right) \cdot \left(\frac{\sigma_e}{G}\right)^n. \quad (24)$$

The creep constants A_o, n, and Q_c are given from short time creep data of copper[17]. Material constants used in calculation is listed in Table 1. As stated in section 4, even if the test temperature is elevated, two types of creep; high temperature (HT) and low temperature (LT) creep contribute to the void shrinkage process[17,18]. Therefore, we can not ignore LT creep when we compare the experimental results with calculated ones. In fact, we did not take account of HT creep but also LT creep in Figs. 5 to 7. However, in this section, we only use data of HT creep because we just compare the void change rates (or growth rates of bonded area) calculated by the models.

Now, let us discuss the applicability of the recent models introduced in section 5. **Figures 8** and **9** compare the calculated results of the analytical recent models with that of the finite element method (FEM). Figures 8 and 9 are drawn about dV/dt and dS/dt, respectively. The ratio of h/w is kept constant ($= 0.1$). The boundary condition and initial mesh pattern used for FEM has already been shown in Fig. 3 (a). In this section, two kinds of boundary conditions are adopted again; a perfect constraint ($\dot{\varepsilon}_\infty = 0$) and an uniform deformation ($\dot{\varepsilon}_\infty = \dot{\varepsilon}_p$). The displacement rate $\dot{u}_x$ at $x = L$ was given as shown in Fig. 3 (a). The mesh pattern deformed to $S = 50\%$under the constraint condition has been shown in Fig. 3 (b). As can be seen in (b), the folding process produces the void crushing effect. In spite of the folding phenomenon, the ratio of h/w was not so changed from the initial value of h_o/w_o, when half the dihedral angle at void tip, α_o, was less than 30°. However, in the FEM model, both values of dS/dt and dV/dt became very large immediately after a surface nodal point was folded to the x axis. Therefore, we first estimated the void shrinkage process with time, subject to the initial condition of $S_o = 10\%$ and $h_o/w_o = 0.1$. We did not directly calculated the rates. We obtained the values of dS/dt and dV/dt by smoothing S-t and V-t curves, respectively.

As can be seen in Figs. 8 and 9, the results of FEM for $S < 50\%$ are scarcely influenced by the constraint condition. On the other hand, in $S > 50\%$, if bulk is perfectly constrained, both of dV/dt and dS/dt are reduced more quickly as S increases, compared with those of uniform deformation. It is found that two dotted lines of ● and ▲ approach the curves of FEM. This suggests that both of Takahashi's model (eq. (1)) and Guo and Ridley's model (eq. (8)) are applicable to the bonding process when bulk is uniformly deformed. We need just to alter the value of creep constant A_o so that we can predict the boding process exactly. However, when the bulk is constrained by the bonding jig as S increases or when the void shrinkage process is performed by HIP sintering, eqs. (1) and (8) is not valid at $S > 50\%$. We should use eq. (2) of Takahashi's model in order to predict the bonding process where the bulk is constrained as S increases ($S > 50\%$).

Hancock's model gives $\dot{V}$ smaller than other crushing models in the range of $S < 50\%$. This is caused by no crushing effect of Hancock's model. The difference between Hancock and other models is distinguished by the crushing effect. It is found from Figs. 8 and 9 that Hancock's model is not applicable to predict the change in S. We need to remember that Hancock's model is for $L >> w$[13], that is, Hancock's model is valid for the shrinking process of an isolated void. The results of Hancock's model are in fault for the void arranged in a regular interval of $L \sim w$. Hancock's model requires the uniform bulk deformation. We cannot keep L constant. However, if $L >> w$, we can treat L as a constant, that is , Hancock's model is just applicable around $S = 100\%$. In other words, the results of Hancock's model can approach that of the FEM model as S becomes 100%.

In fact, it is thought that the real void shrinkage rate by power law creep is in the area surrounded by the dotted curves of ▲ and ● in Fig. 8 because the bulk is constrained somewhat by a bonding jig and so on. Therefore, it is concluded that Takahashi's model is applicable when the constraint of the jig is strong, but Guo and Ridley's model is for no constraint condition. We can say that both of them can be used when $S <$ 50%. The authors consider that the equivalent strain rate and constraint condition matters in estimating the void shrinkage rate. In the bonding process under a constant load, the bonding pressure usually decreases as the test specimen (bulk) is deformed. Therefore, we need to take account of the change in the value of P in order to predict the bonding process exactly. However, all models recently developed have not considered it. The FEM model is applicable for all external conditions as long as the visco-plastic deformation is dominant[19,20,21].

7. Conclusions

We have developed a finite element model for the solid state bonding by viscoplastic (creep) deformation. We have further discuss the validity of recent void shrinkage models based on power law creep. We have found that we fail to predict the bonding process, if we use them having no idea, because they have merits and demerits. The present paper has suggested what boundary condition is correct for each model. The main results obtained from the discussion are summarized as follows;

1) The finite element model can predict the solid state bonding process regardless of the external constraint condition.

2) Takahashi's model is applicable for the solid state bonding in the latter stage of which the bulk is constrained.

3) Guo and Ridley's model is valid when the specimen is uniformly deformed. Therefore, it should not be applied to hot isostatic pressure bonding.

4) Hancock's model can be applied only to the shrinkage (or growth) process of an isolated void (at $L > > w$). The difference in volume change rate between Hancock's and Takahashi's models can be explained by the crushing effect due to the voids arranged at regular intervals.

5) When we have the bulk constrained, we should use eq. (2) in predicting the void shrinkage process of $S > 50\%$.

References

1) B.Derby and E.R.Wallach: Metal Sci., 1982, **16**, 49-56.
2) E.Arzt, M.F.Ashby and K.E.Easterling: Metall.Trans., 1983, **14A** , 211-221.
3) K. Nishiguchi and Y. Takahashi: in Proc. Conf. 'Quality and Reliability in Welding' Hangzhou, Sept., 1984, Chinese Mech. Eng. Soc. A-13-1.
4) Idem: Quartery J. Jnp Weld. Soc., 1985,**3** , (2), 303-316, (in Japanese).
5) C.H.Hamilton: in 'Titanium Science and Technology' (ed. R.I.Jaffee and H.M.Burte), 625-648; 1973, New York, Plenum Press.
6) Z.X.Guo and N.Ridley: Mater. Sci. Technol., 1987,**3** , 945-953.
7) H. Yan and M. Longxiang: in 'Superplasticity and Superplastic Forming',(ed. C. Hamilton and N. E. Paton), 513-516; 1988, The Minerals Met. & Mater.Soc.
8) A.Hill and E.R.Wallach: Acta Metall., 1989,**37**, (9), 2425-2437.
9) Y. Takahashi and K. Nishiguchi: Weld. in the World, 1989,**27**, (3/4), 100-113.
10) D.S. Wilkinson and M.F.Ashby: Acta Metall., 1975, **23**, 1277-1285.
11) G.Garmong, N.E.Raton and A.S.Argon: Metall. Trans., 1975, **6A**, 1269-1279.
12) J.W. Hancock: Met. Sci., 1976,**10**, 319-325.
13) F.A.McClintock: J. Applied Mech. ASME, 1968,**35**, 363-371.
14) J.Pilling, D.W.Liversey, J.B. Hawkyard and N. Ridley: Met. Sci., 1984,**18**, 117-122.
15) K.Nishiguchi, Y.Takahashi and T. Koguchi: Doc.RW-368-87,(1987) Resistance Welding Committee in Jpn Weld. Soc. (in Japanese).
16) Y. Takahashi, F. Ueno and K. Nishiguchi: Acta Metall., 1988,**36**,(11),3007-3018.
17) M. Pahutovà, J. Cadek and P. Pys: Phil. Mag., 1973,**23**,509-517.
18) R. Lagneborg: in 'Creep and Fatigue in High Temperature Alloys' (ed. J. Bressers), 1981, Applied Sci. Publishers LTD, London, 41-71.
19) Y. Seguchi, H. Kitagawa and Y. Tomita: in 'Fundamental in Finite element Method', Nikkan Kougyo Newspaper, 1983, Tokyo, 105-110 (in Japanese).
20) Y. Tomita and R. Sowerby: Int. J. Mech. Sci., 1978, **20**, (6),361-371.
21) K. Nishiguchi, Y. Takahashi and T. Koguchi: in Proc. National Spring Meeting, Jpn. Weld. Soc., **40**, 1987, 148-149.
22) V.W. Köster: Zeit Metall. 1948,**39**, (1), 1-9.